Strain relaxation by coherent three-dimensional islanding in molecular-beam epitaxy of EuTe on PbTe(111)

G. Springholz and G. Bauer
Institut für Halbleiterphysik, Johannes Kepler Universität Linz, A-4040 Linz, Austria
(Received 2 February 1993)

By use of *in situ* reflection high-energy electron diffraction (RHEED), the heteroepitaxial growth of strained-layer EuTe on PbTe(111) was investigated. From the determination of the in-plane EuTe surface lattice constant as a function of the layer thickness, the onset of EuTe strain relaxation (at critical layer thickness h_c) was obtained. Time-dependent intensity measurements of different features in the RHEED patterns indicate that the critical layer thickness essentially coincides with an abrupt roughening of the EuTe surface. In spite of the observation that for certain growth conditions a change in the damping of the RHEED intensity oscillations occurs at h_c, generally, the damping behavior does not lead to the correct critical layer thickness. With increasing substrate temperatures, we not only observe a strong increase in the adatom surface diffusion lengths indicated by the damping of the RHEED intensity oscillations, but also a drastic *decrease* in the EuTe critical layer thickness. These facts indicate that the mechanism of initial strain relaxation is due to formation of coherent three-dimensional (3D) islands on the surface and their relaxation by *elastic* lateral deformation. Based on these results, we propose a new interpretation for the limits of 2D layer-by-layer heteroepitaxial growth of EuTe on PbTe(111), the limits being mainly a result of the strain-induced tendency toward 3D islanding on the surface.

I. INTRODUCTION

Advances in molecular-beam epitaxial (MBE) growth techniques have recently led to the fabrication of lead salt heterostructure quantum-well diode lasers.[1] In such structures, PbTe is usually used for the quantum wells, and the ternary $Pb_{1-x}Eu_xTe$ with $x<0.05$ for the barriers. Recently, also PbTe/EuTe superlattices, which represent a combination of a narrow band gap (PbTe, $E_g=190$ meV) and a wide band gap (EuTe, $E_g=2.0$ eV) material, have been used in such structures,[2] as well as in PbTe-EuTe transistor structures.[3] With this new combination of materials, very large confinement energies of the order of 1 eV can be achieved in quantum-well (QW) structures. The EuTe/PbTe system has also attracted attention because of the interesting combination of diamagnetic (PbTe) and antiferromagnetic (EuTe) materials.[4,5] EuTe itself is of interest because a magnetic-field-induced metal-insulator transition has been observed.[6]

PbTe and EuTe crystallize in the rocksalt crystal structure with a lattice mismatch of only 2.1% at room temperature, which still offers good prospects for heteroepitaxial growth. The background doping level in IV-VI compound epitaxial layers is never significantly below 10^{17} cm^{-3} as a consequence of their degree of off-stoichiometry, resulting in lattice vacancies and interstitials acting as donors or acceptors.[7] Therefore, EuTe has potential as an epitaxial insulating layer in IV-VI heterostructures in order to separate the active parts of such heterostructures from the parallel conducting buffer layers and substrates, which is, for example, important for the growth of two-dimensional (2D) electron-gas structures.

For the growth of high mobility strained heterostructures, the number of defects in the active layers have to be kept as low as possible. When including highly strained EuTe layers in such structures, the knowledge of the critical EuTe layer thickness h_c for the MBE growth on relaxed PbTe or $Pb_{1-x}Eu_xTe$(111) epitaxial layers is of crucial importance. For single PbTe epilayers on BaF_2(111), we have recently demonstrated the MBE growth of very high mobility films, with Hall mobilities of up to 1.98×10^6 cm^2/V s at 5 K.[8] In addition, we have grown PbTe/EuTe superlattices with remarkable structural perfection, showing up to 18 superlattice satellite reflections in the $\Omega/2\Theta$ x-ray-diffraction curves.[9] This indicates that very smooth and abrupt heterointerfaces can be achieved.[10]

In situ reflection-high-energy electron diffraction (RHEED) has been successfully used to study the critical layer thicknesses h_c for strained layer systems like $In_xGa_{1-x}As$/GaAs,[11–14] $In_xGa_{1-x}As$/InP,[15–17] and Ge/Si.[18] However, no such study has been reported for IV-VI strained layer structures. In this work, we use RHEED to determine the critical layer thickness and investigate the process of subsequent strain relaxation of EuTe grown by MBE on PbTe(111). In addition, we show that the onset of strain relaxation essentially coincides with distinct changes in the RHEED patterns, corresponding to a surface roughening at h_c. The critical thickness is found to depend strongly on the substrate temperature. This indicates that the mechanism of strain relaxation is due to coherent three-dimensional (3D) islanding[13–16] of the strained EuTe layer surface.

II. EXPERIMENT

Our experiments were carried out in a Riber MBE growth chamber with custom-built preparation and load-lock chambers. For PbTe growth, we use a PbTe compound effusion cell, and an additional Te_2 effusion cell for the fine adjustment of the beam flux composition.[8] For EuTe growth, the constituents are evaporated from separate Eu and Te_2 effusion cells.[9] The absolute beam flux rates from the different effusion cells were measured with a quart-crystal thickness monitor, which was also used to calibrate the ion gauge beam flux monitor.[19] The substrate temperatures were calibrated with the melting points of different metals and with the observation of the Te_2 condensation points for calibrated impinging Te_2 flux rates. *In situ* RHEED surface studies were performed with an electron gun operated at 35 keV. The RHEED patterns were recorded with a video camera and further analyzed with a personal-computer-based image-processing system. With this system, up to eight different variable size windows can be positioned onto the RHEED image in order to determined RHEED profiles, or the time evolution of integral intensities of various features in the RHEED patterns.

In our studies, first a thick PbTe buffer layer of about 4 μm was deposited at a substrate temperature of $T_s = 350\,^{\circ}C$ onto freshly cleaved (111) BaF_2 substrates (lattice mismatch of 4.2% with respect to PbTe). This ensures complete strain relaxation of the PbTe buffer and high structural perfection [full width at half maximum (FWHM) of typically 30 arsec in the x-ray rocking curves],[8] and a very smooth layer surface, in spite of the 3D nucleation of PbTe on BaF_2(111). In detailed strain analysis studies using high-resolution x-ray diffraction of the symmetric (222) and the oblique (246) Bragg reflections, we have found that for such thick PbTe buffer layers the residual strain from the growth on the lattice-mismatched BaF_2 substrates is much below 0.08%. In general, no clear surface reconstruction of the PbTe(111) surface is observed, except after long-term annealing and subsequent cooling to low substrate temperatures. Then weak half-order streaks in the sixfold $[1\bar{1}0]$ directions appear in the RHEED patterns.[19]

EuTe was grown on the PbTe buffer at growth rates of about 0.45 monolayers/sec [=1.7 Å/sec, 1 monolayer (ML) EuTe=3.82 Å], which is given by the impinging Eu flux rate and was also determined from RHEED intensity oscillations. Te_2 flux rates of the order of 1 ML/sec [1 ML/sec is equivalent to 5.54×10^{14} atoms/cm^2 sec for the PbTe(111) surface] were used, which corresponds to a Te_2-to-Eu flux ratio of about 2. The substrate temperatures ranged from 250 to 310 °C. Under such growth conditions 2D nucleation and 2D growth of EuTe on PbTe(111) occurs.[9,20] Two different surface reconstructions of EuTe(111) corresponding to a Te-stabilized surface and a Eu-stabilized surface have been observed.[9] With a Te_2-to-Eu flux ratio of 2 and a substrate temperature above 260 °C, the growing EuTe surface is Eu stabilized with a $(2\sqrt{3}\times2\sqrt{3})R30^{\circ}$ surface reconstruction. This is evidenced by the appearance of $\frac{1}{2}$-order streaks in the RHEED pattern for the $[1\bar{1}0]$ and the $[\bar{3}21]$ azimuths, and of $\frac{1}{6}$-order streaks in the $[1\bar{2}1]$ azimuths. For lower substrate temperatures, the growing surface is Te stabilized, indicated by the observation of a multidomain (3×4) surface reconstruction with $\frac{1}{3}$- and $\frac{1}{4}$-order streaks in the $[1\bar{1}0]$ azimuths, $\frac{1}{6}$-order streaks in the $[\bar{3}21]$ azimuths, and weak $\frac{1}{2}$-order streaks in the $[1\bar{2}1]$ azimuths.

III. CRITICAL LAYER THICKNESS DETERMINATION

In the first set of experiments, the heteroepitaxial growth of EuTe on PbTe(111) was monitored by RHEED in the $[1\bar{1}0]$ azimuth and the images were recorded on video tape for further analysis. The angle of incidence of the electron beam was set to 1.2°, so that the (02) and $(0\bar{2})$ streaks appeared just above the shadow edge. The growth rate was 0.45 ML/sec (=1.7 Å/sec) and the Te_2 flux rate was 0.88 ML/sec (Te_2-to-Eu flux ratio of 1.92). The substrate temperature of 260 °C is about 35 °C above the Te_2-condensation point (which is used as a temperature reference point) resulting in the Eu-stabilized growth mode.[9] In order to determine the in-plane lattice constant of the growing surface, RHEED intensity profiles parallel to the shadow edge were measured periodically after every 2–5 ML up to a total layer thickness of 275 ML (=1050 Å). To achieve a high resolution for the spacing of the diffraction streaks, the window in which the intensity profiles were measured was set close to the shadow edge (about 0.3° away) in order to include the outmost streaks of the RHEED image. Examples of the measured profiles at different stages of the EuTe growth are shown in Fig. 1 for the initial PbTe surface (top trace) and for EuTe layer thicknesses of 4, 20, 41, 47, 81, 148,

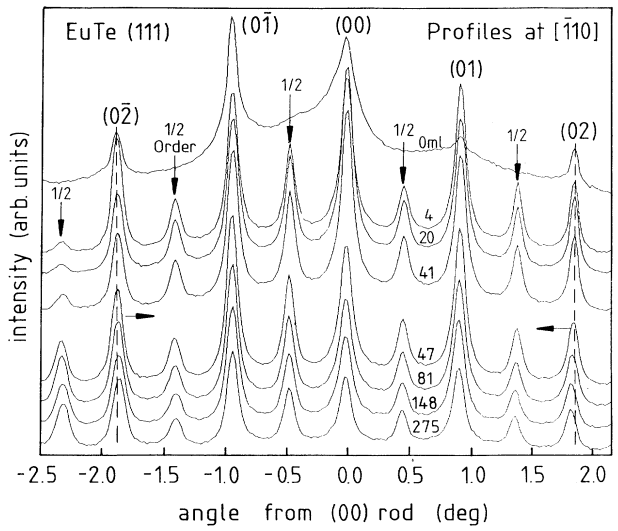

FIG. 1. RHEED profiles ($[1\bar{1}0]$ azimuth) parallel to the shadow edge for a EuTe layer on PbTe(111) as a function of the layer thickness. From top to bottom: the initial PbTe surface, then the EuTe surface after deposition of 4, 20, 41, 47, 81, 148, and 275 monolayers (1 ML=3.82 Å). The critical EuTe layer thickness is determined to be 45 ML.

and 275 ML (traces from the second from the top to the bottom in Fig. 1). Note the additional $\frac{1}{2}$-order streaks due to the EuTe $(2\sqrt{3}\times 2\sqrt{3})R30°$ surface reconstruction. As indicated in Fig. 1, the streak separation for the EuTe surface is initially constant and identical to that of the PbTe surface, up to a EuTe layer thickness of roughly 45 ML; then, however, it starts to decrease, indicating an increase (relaxation) of the EuTe surface lattice constant.

The relaxed bulk lattice constant of EuTe is 6.598 Å at room temperature and 6.619 Å at the growth temperature of $T_s = 260\,°C$, taking into account the linear thermal expansion coefficient of $\beta_{\text{lin},300\text{ K}} = 13.6\times 10^{-6}\ \text{K}^{-1}$ for EuTe.[21] PbTe has a bulk lattice constant of 6.462 Å at room temperature, and of 6.492 Å at 260 °C, with a thermal expansion coefficient of $\beta_{\text{lin},300\text{ K}} = 20\times 10^{-6}\ \text{K}^{-1}$.[22] This results in a compressive lattice mismatch of 1.95% at $T_s = 260\,°C$. Because of the smaller thermal expansion coefficient of EuTe as compared to PbTe, the lattice mismatch at the elevated growth temperature is somewhat smaller than the lattice mismatch of 2.1% at room temperature. The angular scale in Fig. 1 was obtained by using the peak spacing for the PbTe surface with the known (111) surface lattice constant of $a_0 = 4.591$ Å as a reference. For the very small scattering angles involved, to a good approximation the actual in-plane EuTe surface lattice constant is given directly by the ratio of the streak separation for the PbTe surface to that of the EuTe surface multiplied by the PbTe surface lattice constant a_0. The angular resolution is limited by the number of pixels (equal to the number of data points) between the different peaks in the profiles, and is, in our case, 0.0086°. Therefore relative changes in the surface lattice constant can be resolved within 0.24%.

The result of the in-plane EuTe surface lattice constant as a function of the layer thickness is presented in Fig. 2. The in-plane lattice constant a_s (left scale) is expressed in terms of the corresponding bulk EuTe in-plane lattice constant, which is just $\sqrt{2}$ times the (111) surface lattice constant. The corresponding in-plane strain $[(a_s - a_{0,\text{EuTe}})/a_{0,\text{EuTe}}]$ is shown on the right-hand scale of the graph. As indicated, up to a layer thickness of 45 ML (=182 Å), the actual in-plane lattice constant of the EuTe layer is equal to the lattice constant of the relaxed PbTe buffer layer, with the maximum in-plane strain value of $\varepsilon_{\parallel} = -1.916\%$. Beyond this, the EuTe in-plane lattice constant starts to increase, indicating the onset of strain relaxation, at first quite rapidly, but after 80 ML more slowly. Even after the growth of 300 ML, the EuTe layer is still not yet fully relaxed, with a residual strain of −0.5%.

For the given growth conditions the critical layer thickness is determined to be 45 ML or 182 Å, with an uncertainty of ±4 ML or ±16 Å. For comparison, we calculated the critical layer thickness for this material system according to the Matthews-Blakeslee model,[23] taking the EuTe elastic constants given in Ref. 21 and assuming a similar misfit dislocation formation mechanism as found for PbTe.[24] With these assumptions, we get a Matthews-Blakeslee critical EuTe layer thickness of only $h_c^{\text{MB}} = 12$ ML or 46 Å, which is about a factor 4 smaller than what we found experimentally. This is quite typical

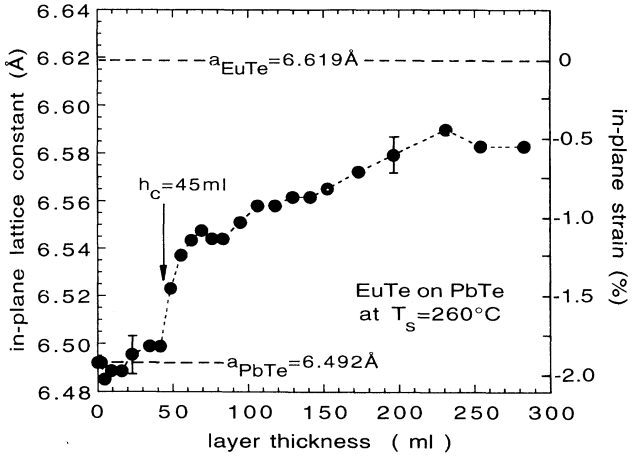

FIG. 2. In-plane surface lattice constant (left scale) and in-plane strain $\varepsilon_{\parallel}$ (right scale) of EuTe on PbTe(111) as a function of the EuTe layer thickness, obtained from an analysis of the RHEED profiles shown in Fig. 1. The bulk lattice constants at $T_s = 260\,°C$ are 6.492 Å for PbTe, and 6.619 Å for EuTe, resulting in a maximum strain value of $\varepsilon_{\parallel} = -1.916\%$ for the fully strained EuTe layer. The onset of strain relaxation (arrow) occurs at a critical layer thickness of $h_c = 45$ ML or 172 Å±4 ML.

for strained layer MBE growth, where the experimentally observed critical layer thicknesses are usually significantly larger than predicted according to Matthews-Blakeslee.[11–14,25]

IV. SURFACE ROUGHENING AT THE CRITICAL LAYER THICKNESS

The sequence of the $[1\bar{1}0]$ RHEED patterns at the different stages of EuTe growth, for the growth described above, is depicted in Fig. 3. Figure 3(a) shows the RHEED pattern of the initial Pb-stabilized PbTe surface, revealing its very high degree of structural perfection. This is evidenced by the sharp, almost point-shaped diffraction streaks with the very bright diffraction spots all arranged on the semicircle of the zeroth-order Laue zone. This can be observed only for very perfect 2D surfaces.[26,27] In addition, the sharp and bright Kikuchi lines across the RHEED pattern indicate a high crystalline perfection.[28]

As soon as the growth is started, the RHEED pattern changes drastically [Fig. 3(b) after the growth of 1-ML EuTe]. The diffraction streaks are considerably elongated and broadened, which indicates a broadening of the reciprocal lattice rods[26,27] due to an increasing surface disorder in the nucleation stage, which also results in an increase of the diffuse background intensity. However, since no 3D transmission features (i.e., transmission diffraction *spots*) appear in the RHEED patterns, a true 2D nucleation of EuTe on the PbTe surface occurs, in spite of the considerable lattice mismatch. Additionally, the $\frac{1}{2}$-order diffraction streaks of the $(2\sqrt{3}\times 2\sqrt{3})R30°$ EuTe surface reconstruction are already well developed within the growth of only 1 ML.

As growth continues, the diffuse background intensity in the RHEED patterns decreases, the streaks sharpen,

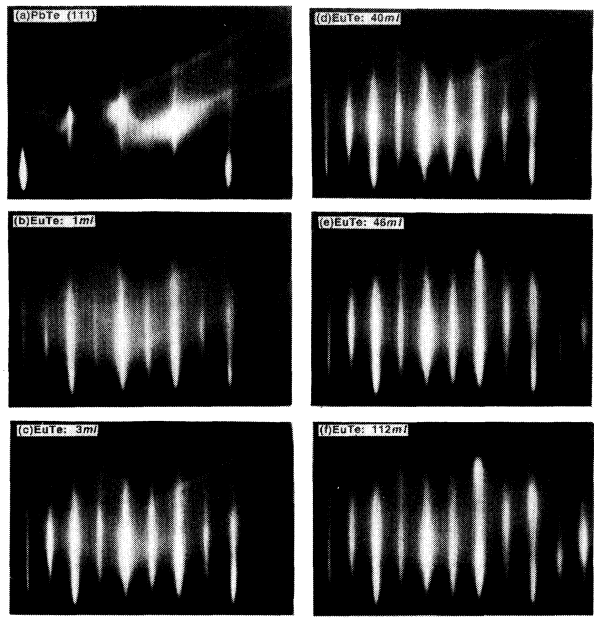

FIG. 3. RHEED patterns of EuTe on PbTe(111) at different stages of growth: (a) for the initial PbTe surface; (b) after 1 ML EuTe, (c) after 3 ML EuTe, (d) after 40 ML EuTe (just before the critical layer thickness $h_c = 45$ ML); (e) after 46 ML EuTe (just after $h_c = 45$ ML); and (f) after 112 ML EuTe. Diffraction conditions: [1$\bar{1}$0] azimuth and angle of incidence of 1.2°.

and the Kikuchi lines partially recover. The presence of Kikuchi lines indicates the perfect epitaxial relationship of the strained EuTe layer to the PbTe buffer. In the (111) EuTe layer, the crystal lattice is rhombohedrally distorted due to the biaxial strain induced by the lattice mismatch to PbTe buffer. Therefore, subsurface lattice planes in the EuTe layer and the PbTe buffer which are tilted relative to the (111) surface are no longer exactly parallel to each other. As a result, the Kikuchi electrons scattered from these planes are no longer reflected in the same scattering angles, and their constructive Bragg interference is reduced. This explains the weakening and diffuse appearance of the Kikuchi lines in the RHEED patterns.

After only three EuTe monolayers [Fig. 3(c)] the transformation from the unreconstructed PbTe surface to the reconstructed EuTe surface is completed, and the RHEED pattern does not change during the growth of the subsequent 37 ML [see Fig. 3(d), RHEED pattern after 44 EuTe monolayers]. Then, however, within only few monolayers, the RHEED pattern changes abruptly [compare Fig. 3(d) at 40 ML and Fig. 3(e) at 46 ML]. Clearly, at $d = 46$ ML ($\approx h_c$) the Kikuchi lines disappear and the diffraction streaks become spotty, indicating the onset of a surface roughening. When growth is further continued, the RHEED pattern does not change much more [see Fig. 3(f) at 112 EuTe monolayers] and no reimprovement of the surface is observed. Although even the higher fractional order Laue zones can be observed in the RHEED patterns, the EuTe surface is considerably more disordered than the PbTe surface, since for the EuTe surface we have never observed such sharp diffraction spots as those arranged on the zeroth-order Laue semicircle shown in Fig. 3(a). Note that from the comparison of the RHEED patterns for PbTe and EuTe surfaces, it is clear that the strong streaking for the EuTe surface does not result from an instrumental broadening.

In order to investigate the changes in the RHEED patterns at the critical EuTe layer thickness in more detail, the contributions from the different diffraction processes have to be sorted out. Apart from the specular spot, we focused on three main diffraction features: (1) the diffraction spots or streaks originating from scattering from the perfect 2D surface, including the fractional order streaks; (2) bulk 3D diffraction spots arising from the Bragg diffraction of electrons transmitted through surface asperities or three-dimensional islands; and (3) Kikuchi lines, which are a result of diffuse, inelastic low-energy-loss scattering events and subsequent Bragg reflections from subsurface atomic planes in the epilayers.[28]

In Fig. 4, a schematic representation of the RHEED images of Fig. 3 is depicted, showing the exact positions of the different diffraction features. The ideal 2D integer order diffraction spots (large dots in Fig. 4 with 2D indices) on the zeroth-order Laue circle (dashed semicircle) and the positions of the Kikuchi lines (dash-dotted lines

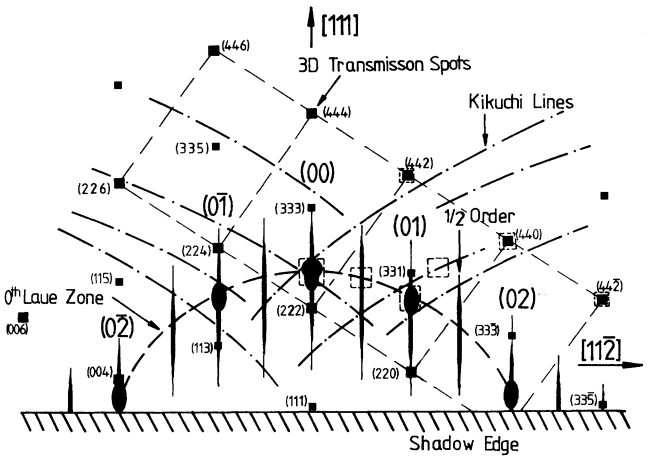

FIG. 4. Schematic representation of the [1$\bar{1}$0] RHEED patterns shown in Fig. 3, indicating the positions of the different diffraction features. Large spots on the dashed semicircle indicate diffraction spots from an ideal 2D surface lying on the zeroth-order Laue circle (dashed semicircle) as observed for the PbTe surface [Fig. 3(a)]. Vertical lines are the elongated diffraction streaks for a disordered 2D surface (EuTe surfaces [Figs. 3(b)–3(f)]), with the additional $\frac{1}{2}$-order streaks of the $(2\sqrt{3}\times 2\sqrt{3})R30°$ surface reconstruction. Dash-dotted lines: Kikuchi lines; full squares: 3D Bragg transmission diffraction spots with corresponding 3D indices, observed for the rougher EuTe surfaces beyond the critical layer thickness [Figs. 3(e)–3(f)]. Small squares: low intensity; larger squares: high intensity spots. The open dashed squares represent the windows for the time-dependent intensity measurements shown in Fig. 5.

in Fig. 4) were obtained from the RHEED pattern of the PbTe surface [Fig. 3(a)]. The more disordered EuTe layer surface results in strongly elongated integral and half-order streaks (indicated by vertical lines in Fig. 4), so that the semicircle of the zeroth-order Laue zone can no longer be clearly resolved. The 3D transmission spots which appear in the RHEED pattern upon surface roughening are represented by full squares in Fig. 4 and are marked with 3D indices. The larger squares with even-number indices refer to high intensity 3D diffraction spots, the smaller squares with odd-number indices to lower intensity. The 3D diffraction spots lie only on *integer* 2D diffraction streaks, which causes the spotty appearance of the streaks when surface roughness is present. It should be stressed that it is important to distinguish between the bright spots on the streaks caused by the superposition of 3D transmission spots and those bright spots which are the result of the crossing of a Kikuchi line and a diffraction streak. The latter effect is known to strongly enhance the streak intensity at the crossing points.[29] In contrast to the 3D spot superposition, present only along the integral order streaks, the latter effect occurs on the integral as well as the fractional order streaks.

Windows were positioned around different RHEED features for time-dependent integral intensity measurements. The results are shown in Fig. 5 for (from top to bottom) the specular spot; the (01) streak and the (0 $\frac{1}{2}$) streaks at the Laue circle positions; an isolated Kikuchi line; and the (44$\bar{2}$), (442), and (440) 3D transmission spots, which are located on the (01), (02) and (03) streaks, respectively. The positions of the corresponding measurement windows are indicated by open-dashed squares

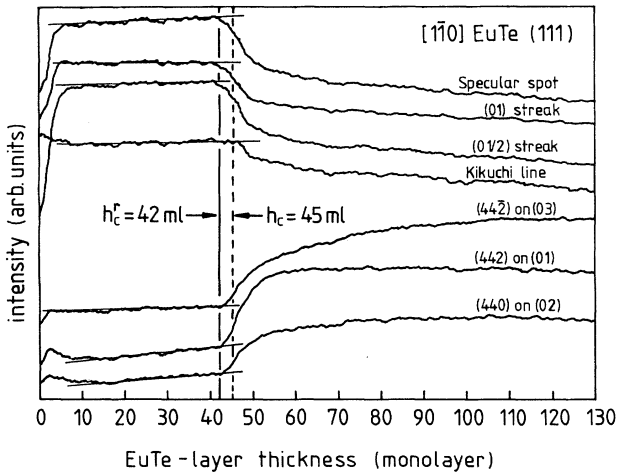

FIG. 5. Intensities of different features in the RHEED patterns as a function of the EuTe layer thickness. Traces from top to bottom: specular spot intensity; intensity of the (01) streak and the (0 $\frac{1}{2}$) streak at the zeroth Laue circle position; intensity of a single Kikuchi line, and intensities of the (44$\bar{2}$), (442), and (440) Bragg transmission features. h_c indicates the critical thickness obtained from the RHEED profile analysis (Figs. 1 and 2). h_c^r indicates the onset of the surface roughening. The positions of the features are indicated by dashed open squares in Fig. 4.

in Fig. 4. We emphasize that there is not much overlap between the different diffraction features for the chosen diffraction conditions, which is not always the case, causing complications in the interpretation of the RHEED intensities.

Apart from the initial intensity changes in the RHEED patterns, when the EuTe growth is started, the intensities of the different RHEED features of the EuTe surface are nearly constant once the formation of the EuTe surface reconstruction is completed. At $d=42$ ML, however, just before the critical layer thickness of $h_c=45$ ML is reached, a quite abrupt change of the intensities occurs. All features that result from the scattering from an ideal 2D surface [specular spot, (01) and (0 $\frac{1}{2}$) streaks] decrease in intensity and start to saturate about ten EuTe monolayers beyond h_c on a lower intensity level. In contrast, at the positions of the 3D transmission features [the (44$\bar{2}$), (442), and (440)], there is a strong increase of the intensities and a saturation on a much higher intensity level. This indicates that the onset of strain relaxation at h_c is preceded by an abrupt increase in the surface roughness at $h_c^r=42$ ML. However, the disappearance of Kikuchi lines coincides *exactly* with the onset of strain relaxation at $h_c=45$ ML (see arrow, Fig. 5). Since the presence of Kikuchi lines in the RHEED patterns depends crucially on the coherence of the subsurface lattice planes,[28] this disappearance of the Kikuchi lines *directly* indicates the onset of strain relaxation (h_c) when this coherence is lost. Consequently, h_c is not only much more readily deduced from these time-dependent intensity measurements than from the RHEED profile analysis, but is also more precise, since the intensity changes are rather abrupt. In contrast, the change in the in-plane lattice constant is small and smooth, resulting in a comparatively large experimental error because of the limited instrumental resolution.

V. RHEED INTENSITY OSCILLATIONS

In another set of experiments, the RHEED intensity oscillations were studied for substrate temperatures between 250 and 310 °C, i.e., in the regime where 2D nucleation and growth of EuTe on PbTe(111) occurs for the given Te_2 flux rate.[9] We were interested in the relationship between the critical layer thickness and the damping behavior of the RHEED oscillations since, quite commonly, the onset of an additional damping of the oscillations has been used as another criterion for determination of the critical layer thickness.[13,14,17] For the following experiments we used flux rates of 0.475 ML/sec for Eu and 1.24 ML/sec for Te_2, which are only slightly higher than in the previous experiments. In all cases, a thick PbTe layer was grown prior to our RHEED experiments in order to ensure identical starting conditions, i.e., a fully relaxed buffer layer and a smooth surface. We also used different diffraction conditions, namely a smaller angle of incidence of 0.76° and an azimuthal angle of 1.3° off the [1$\bar{1}$0] azimuth, in order to enhance the RHEED sensitivity to changes in the surface step density and to enhance the amplitude of the RHEED intensity oscillations.

In Fig. 6, the intensity oscillations of representative features in the RHEED pattern are shown for $T_s = 270\,^{\circ}\mathrm{C}$. Because of the somewhat higher Te_2 flux rate used in this experiment, this substrate temperature corresponds to the $T_s = 260\,^{\circ}\mathrm{C}$ used in the previous experiments. For the chosen diffraction and growth conditions, well-developed intensity oscillations for different RHEED features with up to 50 oscillations are observed, with some differences in the damping behavior. Again, RHEED features can be divided into two groups: (a) features characteristic (and of high intensity) for the flat 2D surface, namely the streak intensities at the zeroth-order Laue circle position [Fig. 6, from top: (01), (0 $\frac{1}{2}$) streaks and the specular spot]; and (b) features characteristic of a rougher surface, namely the 3D transmission spots away from the Laue circle [Fig. 6, bottom traces: (333) and (113) Bragg reflections]. As shown in Fig. 6, at a EuTe layer thickness of about 45 ML (which is directly obtained from the number of oscillation periods) there is an onset of an intensity decrease for the 2D (01) and the (0 $\frac{1}{2}$) streaks. In contrast, the intensity of the 3D (333) and (113) transmission spots starts to increase. This again indicates a roughening of the EuTe surface at h_c, as discussed above. It should be noted, however, that the observed intensity changes at h_c are clearly smaller than those shown in Fig. 4. We believe that this results from the different choice of diffraction conditions, now optimized in terms of well-developed RHEED oscillations, however also resulting in a greater overlap of different RHEED features. This is especially true for the specular spot, which overlaps with the (222) 3D transmission spot. As a result, the mean intensity at the specular spot position remains essentially constant at h_c, because the decrease of specular spot intensity is partially compensated for by the superimposed increase of the (222) Bragg intensity.

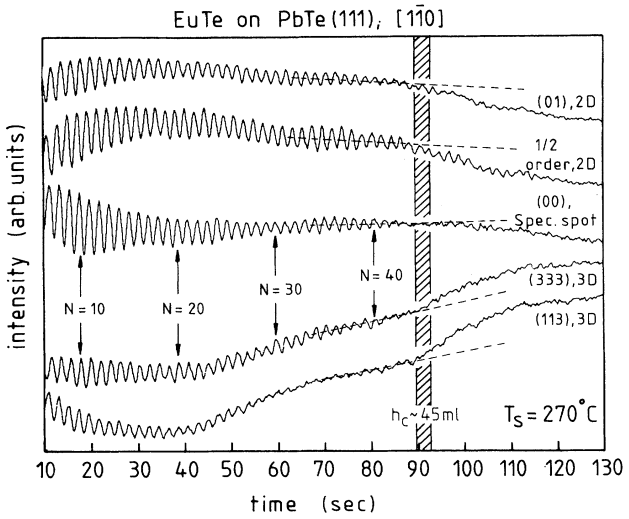

FIG. 6. RHEED intensity oscillations of different RHEED features for strained layer growth of EuTe on PbTe(111). From top to bottom: Intensity oscillations of the (01) streak; the (0 $\frac{1}{2}$)-order streak (both at the zeroth Laue circle position); the specular spot; and the Bragg (333) and (113) transmission spots. The growth condition ($T_s = 270\,^{\circ}\mathrm{C}$, $J_{\mathrm{Eu}} = 0.475$ ML/sec and $J_{\mathrm{Te}} = 1.24$ ML/sec) corresponds roughly to the conditions used in the previous experiments (Figs. 1–5). The critical layer thickness h_c is 45 ML. Because of the different diffraction conditions (1.3° off the [1$\bar{1}$0] azimuth, angle of incidence of 0.76°) the intensity changes at h_c are less well developed than those shown in Fig. 5.

Concerning the behavior of the RHEED oscillations, we observe only a slight increase of the damping at $h_c = 45$ ML. However, this is not very well resolved, since the oscillations are already quite strongly damped before reaching h_c. In the case of the (333) and (113) spots, the oscillations are already totally damped at h_c. In the case of the specular and (01) spots, the oscillations disappears just at the critical thickness h_c. For the (0 $\frac{1}{2}$) spot the oscillations persist even beyond h_c, though with stronger damping. As a result it can be concluded that, in general, for strained heteroepitaxial growth an increasing damping or the disappearance of the RHEED intensity oscillations by itself is not a clear and unambiguous indication of the onset of strain relaxation. The damping of the RHEED oscillations depends mainly on the kinetics and mobility of the surface adatoms and the surface morphology. Consequently, an additional damping of the RHEED oscillations at the onset of strain relaxation can only be expected if a simultaneous change of the surface morphology occurs.

VI. DEPENDENCE OF CRITICAL LAYER THICKNESS AND RHEED INTENSITY OSCILLATIONS ON SUBSTRATE TEMPERATURE

The onset of strain relaxation and the RHEED intensity oscillations were studied as a function of the substrate temperature between 250 and 310 °C for the fixed diffraction conditions, and the Eu and Te_2 flux rates given above. The results are presented in Fig. 7, where the recorded RHEED intensity oscillations of the (00) streak for the different T_s are depicted, with the onset of strain relaxation being indicated by arrows. In all cases, the EuTe growth was started on a fully relaxed PbTe buffer layer freshly grown prior to each experiment. As shown in Fig. 7, a transitional behavior of the RHEED intensities is first observed during the growth of the initial 2–3 EuTe monolayers in which the surface rearranges from the unreconstructed PbTe surface to the reconstructed EuTe pattern, with additional $\frac{1}{2}$-order streaks causing a drastic overall change in the RHEED intensities (Fig. 3). In addition, since the EuTe growth is started on the Te-stabilized PbTe surface (opened Te shutter), the Te-surface coverage decreases when the Eu shutter is opened to start the EuTe growth. When the steady-state EuTe surface is reached after the growth of about 4 ML, the RHEED intensities stabilize on a different intensity level and RHEED oscillations develop. For our diffraction conditions we observe a phase shift of the oscillation of about 180° with respect to the start of growth.

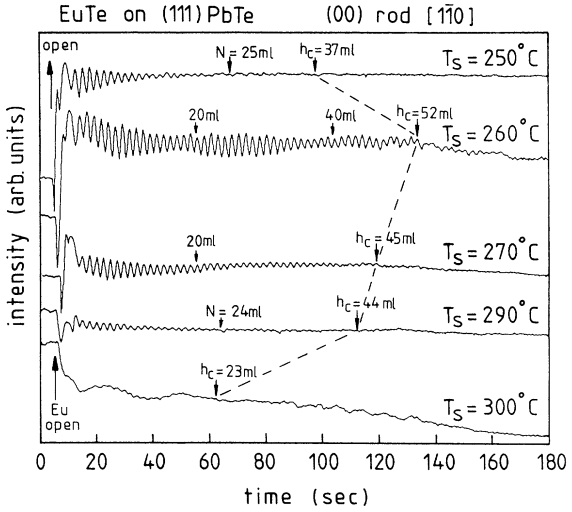

FIG. 7. RHEED intensity oscillations of the (00) streak for strained layer growth of EuTe on PbTe(111) for substrate temperatures between 250 and 300 °C, with constant Eu- and Te_2-flux rates of 0.475 ML/sec and 1.24 ML/sec, respectively. Also indicated are the critical layer thicknesses h_c, as determined from the distinct changes of the intensities of characteristic 2D and 3D diffraction features at h_c as shown in Fig. 5.

As shown in Fig. 7, the amplitude, as well as the damping behavior and the steady-state intensity level of the RHEED oscillations, is *extremely* dependent on substrate temperature. For $T_s = 250$ °C (top trace) and the Te_2-to-Eu flux ratio of 2.65, the growth proceeds in the Te-stabilized mode, whereas for the higher substrate temperatures from 260 to 300 °C (lower traces), the Eu-stabilized growth mode is present. This is indicated by the appearance of the corresponding surface reconstructions. The steady-state RHEED intensity decreases with increasing T_s and reflects mainly the decreasing Te-surface coverage with increasing T_s, similar to our observations for the $Pb_{1-x}Eu_xTe(111)$ surface ($x < 6\%$).[19] The most striking feature in the oscillation traces, however, is the very drastic change in the damping behavior for only very small changes in the substrate temperatures. This is completely different from our observations for MBE growth of PbTe(111), where we have observed well-developed RHEED oscillations for a very wide range of substrate temperature from $T_s = 450$ °C down to room temperature.

For the growth in the Te-stabilized mode ($T_s = 250$ °C), the RHEED oscillations are totally damped already after $N = 25$ oscillation periods. At $T_s = 260$ °C (Eu-stabilized growth) the damping is much weaker and very well-developed RHEED oscillations up $N = 52$ periods are observed and then abruptly disappear, indicating a surface roughening. When T_s is further increased, the RHEED oscillations are much more strongly damped. At $T_s = 270$ °C, $N = 45$ periods are observed. At $T_s = 290$ °C weak oscillations with only $N = 24$ periods can be seen. Finally, at $T_s = 300$ °C, no RHEED oscillations are observed. At even higher substrate temperatures (310 °C and above, not shown in Fig. 7), the heteroepitaxial growth on PbTe changes to a 3D growth mode[8] (see discussion below), so consequently RHEED oscillations are totally absent.

The critical layer thicknesses for the different growth runs were determined from the roughening transition manifested by the intensity changes in the RHEED patterns as described above. We observe a similar behavior for h_c as for the damping of the RHEED oscillations: at low T_s (250 °C) and a Te-stabilized growth we found a critical layer thickness of $h_c = 37$ ML, whereas the RHEED oscillations are already fully damped after $N = 25$ ML. When we change to the Eu-stabilized growth mode at $T_s = 260$ and 270 °C, a much larger h_c of 52 and 45 ML, respectively, is observed. In these cases the RHEED oscillations persist up to h_c and then quickly disappear. With further increasing substrate temperature, the critical layer thickness decreases again to $h_c = 44$ ML at $T_s = 290$ °C and to $h_c = 23$ ML at $T_s = 300$ °C. In addition, the 3D transmission spots observed at the roughening transition become more and more intense, indicating a stronger roughening at h_c with increasing T_s. However, because of the much stronger damping, the RHEED oscillations have already disappeared long before the critical layer thickness is reached. Finally, at $T_s = 310$ °C, no more 2D layer by layer growth of EuTe on PbTe occurs, and the RHEED patterns change after just 2–5 ML EuTe to a full 3D transmission pattern, and therefore no reasonable value for the critical layer thickness could be obtained. It is clear from these results that in general the damping of the RHEED oscillations by itself is not a clear and sufficient indication for the critical layer thickness.

As for MBE growth of GaAs,[30] it is reasonable to assume that for MBE of EuTe the surface kinetics are dominated by the metal (i.e., Eu) surface diffusion lengths, since the growth is mainly limited by the impinging Eu flux rate because of the very high Te_2 redesorption rates. Therefore, we interpret the stronger damping of the RHEED oscillations at higher substrate temperatures in terms of an increase of the Eu surface diffusion lengths. This behavior is not so much caused by an increase of the thermally activated adatom *hopping frequency,* but rather by an increase of the mean Eu adatoms surface diffusion *time* with increasing substrate temperature. This surface diffusion time is determined by the average residential time of Eu adatoms on the surface before forming immobile Eu-Te complexes, or before being incorporated at step edges. It is clear that such Eu-Te complexes are very stable because of the very strong Eu-Te bond, and that their surface mobility is probably orders of magnitudes smaller than that of the single Eu adatoms. This means that once a Eu adatom is incorporated in such a complex, its surface diffusion is essentially stopped.

With increasing T_s, the Te-adatom surface coverage decreases very strongly due to the exponential increase of the Te_2 desorption rate from the surface, and the impinging Eu adatoms have to diffuse much *longer* to encounter free Te adatoms on the surface to form immobile Eu-Te complexes, or to find free Te sites to become incorporated

into the crystal lattice. Consequently, at higher substrate temperatures and lower Te-surface coverages, the mean Eu adatoms surface *diffusion times* and consequently also their mean *diffusion lengths* are much larger than those for the larger Te-surface coverages at lower substrate temperatures. At higher T_s, because of the larger diffusion lengths, adatom incorporation occurs at step edges, and therefore a step-flow growth mode is favored instead of island nucleation and coalescence. This results in a reduced RHEED oscillation amplitude and a faster damping. These arguments are supported by the unusually strong change in the damping of the RHEED oscillations for a change in T_s of only 40 °C—from more than 50 oscillations observed at $T_s = 260$ °C to zero for $T_s = 300$ °C. This cannot easily be explained by considering only a thermally induced increase of the hopping frequency. In such a case, a similarly strong change in the damping behavior is usually expected only for changes in substrate temperatures of the order of 100 °C or more.

For the substrate temperatures below 250 °C, the growth proceeds in the Te-stabilized mode and, compared to the Eu-stabilized growth, the surface properties and growth kinetics seem to be changed completely. Although the initial oscillation amplitude is as high as for the Eu-stabilized mode at $T_s = 260$ °C, the damping of the RHEED oscillations is *increased,* although a *decrease* would be expected from the decrease of the surface diffusion lengths. We suggest a dynamical surface roughening as an explanation for this behavior. The high Te-surface coverages result in a drastically reduced surface adatom mobility. This causes a pronounced surface roughening during growth, resulting in a large steady-state surface step density and a strong damping of the RHEED oscillations. This is indicated by a broadening of the diffraction streaks, a high diffuse background RHEED intensity, and a *gradual* (not abrupt) development of 3D diffraction features after continued growth. Therefore, the critical thickness for surface roughening is not well resolved in this case.

VII. DISCUSSION

A. Strain relaxation by coherent 3D islanding

In this RHEED study of the critical layer thickness for the heteroepitaxial growth of EuTe on PbTe(111), we have shown that within the experimental error, the critical EuTe layer thickness h_c coincides with an abrupt surface roughening. Using *in situ* RHEED, the critical EuTe layer thickness h_c was determined directly by the onset of the in-plane surface lattice constant relaxation, whereas the surface roughening was determined by time-dependent RHEED intensity measurements. The abrupt surface roughening is indicated by an appearance and intensity increase of 3D Bragg diffraction features and by an intensity decrease of the 2D diffraction features which seems to be already completed after the growth of a few monolayers beyond h_c. With increasing substrate temperature, we observe a dramatic decrease of the critical layer thickness, and an increase of the degree of surface roughening.

These observations indicate that the mechanism of initial strain relaxation is via coherent 3D islanding, a model which was recently proposed for heteroepitaxial growth of $In_xGa_{1-x}As$ on GaAs,[13–15] and for Ge on Si.[31,32] This model takes into account that for a strained heteroepitaxial layer exceeding a certain critical thickness "h_c^{3D}," a regularly corrugated surface morphology consisting of 3D islands of multiatomic height can be energetically favorable in comparison to a smooth surface.[13–15,32] In this model, the strain relaxation does not start conventionally by nucleation of misfit dislocations (equivalent to plastic deformation) at the strained layer heterointerface, but rather by *elastic* deformation of the 3D islands formed on the surface. In the case of the islandlike surface, the additional cost of surface energy is overcompensated for by the energy gained from strain relief in the islands by lateral elastic deformation (expansion or compression) of the top layers of the 3D islands, because of free space in between the islands. Only after a significant further increase of the layer thickness does plastic deformation begin by nucleation of misfit dislocations within the 3D islands.[16,31,33] In the following, the layer thickness for the onset of *plastic* strain *relaxation* is denoted by h_c^{pr}, whereas the layer thickness for the onset of *elastic* strain *relaxation* is denoted by h_c^{er}, which in our context is equivalent to the layer thickness of 3D roughening at h_c^{3D}.

The formation of coherent 3D islands depends not only on the strain in the layer but also critically on the growth kinetics and the surface adatoms diffusion lengths, since it is evident that a large adatom mobility is needed for such an extreme rearrangement of the layer surface. As a result, the 3D islanding depends strongly on the growth conditions, i.e., the island formation is enhanced at high substrate temperatures and can be totally suppressed at low substrate temperatures. This explains very well the experimentally observed strong substrate temperature dependence of the critical layer thickness, for example for the growth of $Ga_{1-x}In_xAs$ on InP (Ref. 15) or on GaAs.[12–14] In the case of EuTe on PbTe(111), there is a similar strong dependence of h_c on substrate temperature, h_c decreasing from 52 ML at $T_s = 260$ °C to only 23 ML for $T_s = 300$ °C. At T_s higher than 310 °C, we do not observe 2D but rather 3D growth of EuTe on PbTe, which is now interpreted in terms of a critical layer thickness that has dropped to almost zero. In addition, from the simultaneously observed RHEED intensity oscillations, we found that accompanying the strong change of the critical layer thickness there is a drastic change of the adatom diffusion lengths for changes of T_s as small as 40 °C. This indicates that the critical layer thickness h_c^{3D} is closely related to the growth kinetics at the layer surface.

B. The phase diagram for heteroepitaxial growth of EuTe on PbTe(111)

In Fig. 8 the phase diagram for heteroepitaxial growth of EuTe on PbTe(111) is depicted, showing the dependence of the growth mode and surface structure on the substrate temperature and Te_2 flux rate, for a constant Eu

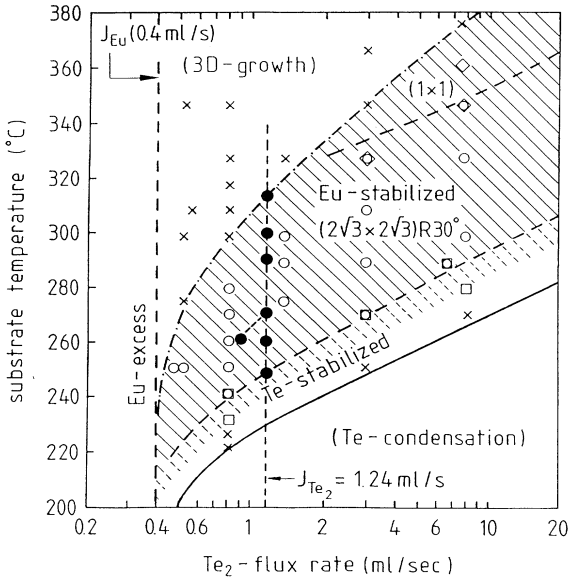

FIG. 8. Phase diagram for strained layer MBE growth of EuTe on PbTe(111) for a wide range of growth conditions, i.e., substrate temperatures and Te_2-flux rates. The Eu-flux rate and the growth rate was kept constant at 0.4 ML/sec. 2D nucleation and 2D layer-by-layer growth occurs only in the dashed region. Below the solid line, Te_2 condensation (crosses) and polycrystalline growth are observed. Above the dash-dotted line 3D epitaxial growth occurs. Within the 2D growth regime, three different EuTe surface reconstructions can be observed; a multidomain (3×4) reconstruction for the Te-stabilized growth mode (squares); a $(2\sqrt{3}\times 2\sqrt{3})R30°$ reconstruction for the Eu-stabilized growth mode (circles), and an unreconstructed (1×1) surface for higher substrate temperatures (diamonds). The growth conditions used for the present work are indicated by the full dots.

flux rate of 0.4 ML/sec. The growth conditions used in the present paper are indicated by full dots. Only in the shaded region in Fig. 8 of the Eu-stabilized growth mode (circles), we observe 2D nucleation and 2D layer-by-layer growth of strained EuTe on PbTe(111). In the Te-stabilized growth mode (squares in Fig. 8), 2D nucleation also occurs, however, followed by a slow steady increase of the surface roughness with increasing layer thickness, eventually leading to 3D growth. At very low substrate temperatures and high Te_2 flux rates (region below the solid line) Te_2 condensation and consequently polycrystalline growth is seen. At high substrate temperatures (crossed above the dash-dotted line), epitaxial, but 3D rather than 2D growth occurs, since the RHEED patterns change within 2–5 ML from an initially streaked pattern to a totally spotty 3D transmission pattern.

Initially, we attributed this upper limit for 2D layer-by-layer growth (dash-dotted line in Fig. 8) to a Te deficiency on the growing surface because of too-large Te_2 redesorption rates at higher substrate temperatures. However, the key point for this discussion is that, in contrast to *heteroepitaxial strained* layer EuTe growth on PbTe(111), for *homoepitaxial unstrained* growth on relaxed EuTe buffer layers 2D layer-by-layer growth without surface roughening is observed up to much higher substrate temperatures. Therefore, the shift of the upper limit for 2D layer-by-layer growth to lower substrate temperatures in the case of *heteroepitaxial* growth of *strained* EuTe on PbTe can only be a result of the strain in the layer. Only this strain acts as a driving force for the coherent 3D islanding and surface roughening, apparently in the extreme case leading to 3D growth already beyond about 2 ML of growth. Thus the region above the dash-dotted line in Fig. 8 can be viewed as the region where the EuTe critical layer thickness h_c^{er} has dropped essentially to zero.

Although the strain in the EuTe layers is the driving force for the 3D islanding, the surface kinetics and adatom mobilities induce additional constraints. Since the damping of the RHEED oscillations reflects the mobility of the surface adatoms, it can be used as an indirect probe for the surface diffusion lengths. The Eu adatom diffusion lengths are strongly determined by the steady-state Te coverage of the surface. The steady-state Te-surface coverage itself is only determined by the dynamical equilibrium between impinging Te_2 flux rate, Te incorporation rate, and Te_2 redesorption rate, where the latter depends exponentially on the substrate temperature. For lower T_s or higher Te_2 flux rates resulting in higher Te-surface coverages, the impinging Eu atoms more easily encounter other free Te adatoms to form strongly bound immobile Eu-Te complexes. This results not only in significantly reduced Eu-adatom diffusion lengths, but also in a reduced tendency for 3D islanding and an increased critical layer thickness as shown in Fig. 7. It is evident that lines parallel to the phase line between Te-stabilized and Eu-stabilized growth modes (dashed line in Fig. 8) represent roughly lines of equal surface coverage and therefore roughly equal adatom diffusion length. Similarly, the upper limit of 2D heteroepitaxy which also runs almost parallel to these lines can be viewed as a line of equal adatom diffusion length. For this "critical" diffusion length (or "critical" Te coverage), the tendency of 3D islanding of the EuTe surface is so strong that no 2D growth can be achieved, reducing the critical layer thickness h_c to almost zero. As an interesting consequence, for all lines of constant Te coverage, an equal critical layer thickness can be expected, independent of substrate temperature and impinging Te_2 flux rate.

At first glance, it seems quite surprising that the critical EuTe layer thickness can drop even below the Matthews-Blakeslee critical layer thickness h_c^{MB} of 12-ML EuTe, since h_c^{MB} usually represents the lowest limit of the critical layer thickness and results from an activationless propagation of preexisting dislocations in the substrate or layer.[23] However, h_c^{MB} is deduced for a homogeneous strain field in a homogeneous layer, which is not present in the case of a 3D islanded surface. In contrast, the onset of 3D islanding depends not only on the strain, but also crucially on the growth conditions (adatom mobility and growth kinetics). Therefore, 3D is-

landing and elastic strain relaxation can start much before the actual onset of plastic relaxation by misfit dislocations at $d \geq h_c^{MB}$. This seems to be the case for EuTe MBE growth on PbTe above the dash-dotted line in Fig. 8. Similar effects have been observed for MBE growth of $In_xGa_{1-x}As$ on InP (Ref. 15) and on GaAs (Refs. 12 and 14) for $T_s \geq 510\,^{\circ}C$ and misfits larger than 2%. It is clear, however, that the actual onset of plastic deformation h_c^{pr}, i.e., formation of misfit dislocations within the 3D islands, should still occur at a layer thickness larger or equal to h_c^{MB}.

Another interesting point to note is that EuTe epitaxial layers on PbTe(111) with a thickness below the critical layer thickness h_c^{3D} are observed to be *metastable*. During and initially after the growth of such a thin layer, sharp diffraction streaks in the [1$\bar{1}$0] RHEED patterns are observed even with visible higher 1/6- and 1/3-order Laue zones of the $(2\sqrt{3}\times 2\sqrt{3})R\,30°$ surface reconstruction. After an annealing of the layer for several minutes at temperatures higher than or equal to the growth temperature, the diffraction pattern becomes spotty and the $\frac{1}{2}$-order streak gradually disappears, indicating the occurrence of a surface roughening and a change to a $(\sqrt{3}\times\sqrt{3})R\,30°$ surface reconstruction. We feel that this surface roughening is the result of a strain-induced coherent 3D islanding of the surface even for the *static* strained EuTe layer. This implies that the mobility of the EuTe surface atoms at the typical substrate temperatures seems already to be high enough that within several minutes of annealing, the static EuTe surface transforms from the initially flat surface to the energetically favorable 3D islanded surface with the minimum free energy. This effect suggests that the critical layer thickness should also depend significantly on the growth rate.

C. Alternative growth models

In a completely different approach, several workers[34–36] have recently proposed alternative models to explain the experimentally observed strong temperature dependence of the critical layer thicknesses. In these models, thermally activated processes for dislocation multiplication[34] or for frictional forces on dislocations[35,36] are proposed in order to explain critical layer thicknesses h_c larger than predicted by the Matthews-Blakeslee (MB) model,[23] as well as the observed substrate temperature dependence of h_c. Within these models, the occurrence of a 2D–3D growth mode transition at h_c is interpreted as being merely induced by the misfit dislocations generated at h_c,[12,35] although no direct experimental evidence for this effect has been given. In contrast, for the case of the Stranski-Krastanov strained layer growth of Ge on Si(100), Eaglesham and Cerullo[31] have shown by transmission electron microscopy (TEM) that the initial 3D Ge islands on Si are totally dislocation free even up to island thicknesses much larger than the critical layer thickness. As for RHEED studies, there is some disagreement whether the onset of 3D islanding precedes,[15] coincides,[11,12] or even follows[37] the onset of surface lattice constant relaxation as determined by RHEED profile analysis. However, it was observed that for growth at higher substrate temperatures h_c^{3D} and consequently h_c^{er} can be significantly smaller than the lowest limit h_c^{MB}.[12,13,15] In such a case it is unrealistic to believe that 3D islands are nucleated by misfit dislocations, since the plastic relaxation is certainly expected to start at a later stage of growth.

On the other hand, the model of coherent 3D islanding by itself does not explain why the experimentally observed critical layer thicknesses can be much larger than those predicted by the Matthews-Blakeslee model. Therefore, for a full understanding of all the experimental data, both the possible 3D islanding, as well as the thermally activated behavior of the misfit dislocations, has to be considered. On the other hand, coherent 3D islanding seems to explain very well the strong temperature dependence of the critical layer thickness, as well as the accompanying morphological changes at the layer surfaces. On the other hand, in the case when 3D islanding is largely suppressed, at low substrate temperatures and/or smaller misfits, the often observed critical layer thicknesses much larger than h_c^{MB} can only be explained by the suppression of nucleation and propagation of dislocations due to energetic barriers. Then the general picture would be the following: for sufficiently low T_s and frozen surface kinetics, 3D island formation and dislocation nucleation is suppressed because of low thermal energies leading to metastable layers with large critical layer thicknesses $h_c^{pr} \gg h_c^{MB}$. This h_c^{pr} is expected to decrease only gradually with increasing growth temperatures. Then for sufficiently high T_s, adatom diffusion lengths, and strain values, coherent 3D islanding starts to occur at critical thicknesses h_c^{3D} smaller than the critical thickness for plastic relaxation h_c^{pr}. Moreover, the resulting critical layer thickness h_c^{er} (elastic relaxation) now decreases very strongly with further increasing T_s because of the increasing tendency of 3D islanding with increasing adatom mobilities. This can lead in the extreme case to an almost zero critical layer thickness.

D. Definition and determination of the critical layer thicknesses

Finally, we would like to address two questions arising from the existence of two different mechanisms of strain relaxation. The first concerns the definition of the critical layer thickness at which strain relaxation begins. Since, conventionally, all surface effects are neglected and the strained layer surface is assumed to be essentially flat, by definition the onset of strain relaxation h_c is equivalent to the onset of plastic deformation (h_c^{pr}) by misfit dislocations. However, if surface effects are also included in the considerations, then *elastic* deformation (h_c^{er}) resulting from morphological changes of the surface (3D islands) become a possible additional mechanism for strain relaxation as well. In such a case, the onset of (elastic) strain relaxation (h_c^{er}) no longer coincides with the onset of

plastic relaxation (h_c^{pr}). As a consequence, now two different critical layer thicknesses should be defined: (1) a critical layer thickness h_c^{er} for strain relaxation by *elastic* deformation caused by changes in surface morphology, and (2) a critical layer thickness h_c^{pr} for strain relaxation by *plastic* or *inelastic* deformation.[15] If surface effects are absent, then only the second critical thickness h_c^{pr} is relevant. If however, depending on epitaxial growth conditions, surface effects are present, then as growth proceeds, first h_c^{er}, corresponding to the onset of 3D islanding, is reached, and at a later stage h_c^{pr}, corresponding to the onset of generation of misfit dislocations within the 3D islands, or even to formation of grain boundaries between adjacent islands. It is clear that the onset of plastic deformation is significantly delayed because in the 3D islands part of the strain is already elastically relieved. In general terms, we propose that the resulting "effective" critical layer thickness h_c should be defined as just the smaller value of h_c^{er} or h_c^{pr}.

The second question concerns determination of the layer in-plane lattice constant using RHEED. In the case of strain relaxation by dislocation formation at the layer heterointerface without change of surface morphology, the *surface* lattice constant is equal to the in-plane lattice constant inside the whole layer. Therefore, by RHEED, which only probes the layer surface, the in-plane strain of the *whole* layer can also be determined. This is not the case if the strain relaxation starts by the formation of 3D islands on the surface and is elastic in nature. Then, a strain *gradient* exists in the elastically deformed 3D islands, with the top atomic layers of the islands being already (partially) relaxed, whereas those at the bottom of the islands and those between the islands may still be fully strained with respect to the substrate or buffer.[14,31] In such a case, the incident electrons are diffracted from areas with different surface lattice constants, and by RHEED a mixture of different surface lattice constants is probed, depending not only on the degree of elastic strain relaxation in the 3D islands, but also on the exact form of surface morphology. In addition, 3D transmission spots superimposed in the RHEED patterns reflect bulklike lattice constants *within* the 3D islands. Therefore, by RHEED it is difficult to extract a well-defined in-plane lattice constant of the layer.

In contrast, the onset of 3D islanding, i.e., the change in surface morphology, can be readily determined. This change should, in principle, coincide exactly with h_c^{er}, since microscopically, as soon as the 3D islands develop they will be partially relaxed. When the contribution from the partially relaxed 3D island surfaces to the RHEED pattern is strong enough, the observed "RHEED" lattice constant will also start to relax, although the onset of plastic strain relaxation at h_c^{pr} may not occur until at a much later stage of growth. The RHEED onset of in-plane surface lattice constant relaxation may not necessarily coincide exactly with the onset of 3D island formation, but can be shifted to somewhat larger layer thicknesses. This is in fact what we have observed in our experiments. Meanwhile, the onset of plastic strain relaxation at h_c^{pr} by formation of misfit dislocations within the islands occurs at a later stage of growth. It is not directly accessible by RHEED, because with this surface-sensitive method a change in the surface lattice constant due either to elastic or plastic deformation cannot be distinguished.

From the practical point of view, in the case of 3D islanding, it is somewhat questionable whether h_c^{pr} is a very meaningful thickness. It has been found that for growth of $In_xGa_{1-x}As$ on InP, strain relaxation by 3D islanding occurs only for lattice mismatches of the order of 2% and larger.[15,16] The critical layer thicknesses h_c^{3D} ($=h_c^{er}$) observed for such large mismatch values are only of the order of a few monolayers, which is much smaller than the critical layer thickness for the onset of plastic relaxation h_c^{pr}. Therefore, before h_c^{pr} is reached, the height of the 3D islands is probably already of the order of the total layer thickness d. This has actually been observed by scanning tunneling microscopy for $In_xGa_{1-x}As$ grown on GaAs,[14] and for Ge on Si by TEM.[31] As a result, the roughness of such a layer with $d \approx h_c^{pr}$ is expected to be comparable to the total layer thickness, which makes the definition of a layer thickness somewhat difficult and arbitrary. Certainly, from the standpoint of epitaxial growth, surface roughening and misfit generation are usually equally detrimental in actual devices. Therefore, the smaller value h_c [often h_c^{er} ($=h_c^{3D}$) and not h_c^{pr}] is of main importance, although for overgrowth the additional knowledge of the larger h_c^{pr} may also be desirable, since for an intermediate layer thickness $< h_c^{pr}$ the elastic strain relaxation should in principle be still reversible.

VIII. CONCLUSIONS

We have investigated the MBE growth and the critical layer thickness of strained EuTe epitaxial layers on PbTe(111) by *in situ* RHEED techniques. Time-dependent intensity measurement of different RHEED features indicates that the onset of EuTe surface lattice constant relaxation (determined by RHEED profile analysis) coincides with a distinct surface roughening. The experimentally obtained critical EuTe layer thickness is strongly dependent on substrate temperature, with a maximum critical EuTe layer thickness of up to 52 monolayers (200 Å) for $T_s = 260\,^{\circ}C$ and a Te_2-to-Eu flux ratio of 2.6. This value is a factor 4 larger than the Matthews-Blakeslee critical layer thickness. The strong temperature dependence of h_c and the accompanying surface roughening can only be understood within the model of coherent 3D island formation. With increasing substrate temperature and increasing Eu-adatom diffusion lengths, the onset of coherent island formation and consequently the critical layer thickness is shifted to much lower values, and at 310 °C is almost zero. This explains the very limited 2D layer-by-layer growth regime for EuTe heteroepitaxial growth on PbTe(111).[9] Therefore, for optimum strained layer growth of EuTe/PbTe heterostructures, the conditions have to be controlled precisely such that the EuTe growth proceeds in the Eu-stabilized growth mode with the substrate temperatures not more

than about 20 °C above the transition to the Te-stabilized mode. For such conditions, we not only observe a large number of RHEED intensity oscillations, indicating a good 2D layer-by-layer growth mode, but also a maximum for the critical EuTe layer thickness and a reduced tendency for surface roughening.

ACKNOWLEDGMENTS

We thank M. Seto for careful reading of the manuscript. Work supported by the Fonds zur Förderung der wissenschaftlichen Forschung, Vienna, Austria (Nos. 7620 TEC and 8446 PHY).

[1]Z. Feit, D. Kostyk, R. J. Woods, and P. Mak, Appl. Phys. Lett. **58**, 343 (1991).

[2]A. Ishida, S. Matsuura, H. Fujiyasu, H. Ebe, and K. Shinohara, Superlatt. Microstruct. **2**, 574 (1986).

[3]D. L. Partin, J. Heremans, C. M. Thrush, L. Green, and C. H. Olk, Phys. Rev. B **38**, 3549 (1988).

[4]J. Heremans and D. L. Partin, Phys. Rev. B **37**, 6311 (1988).

[5]A. Mauger and C. Godart, Phys. Rep. **141**, 51 (1986).

[6]J. Stankiewicz, S. von Molnar, and F. Holtzberg, J. Magn. Magn. Mater. **54-57**, 1217 (1986).

[7]See, for example, *Physics of IV-VI Compounds and Alloys,* edited by S. Rabii (Gordon and Breach, New York, 1974).

[8]G. Springholz, G. Bauer, and G. Ihninger, J. Cryst. Growth **127**, 302 (1993).

[9]G. Springholz and G. Bauer, Appl. Phys. Lett. **62**, 2399 (1993).

[10]V. Holy, J. Kubena, and K. Ploog, Phys. Status Solidi B **162**, 347 (1990).

[11]G. L. Price, Appl. Phys. Lett. **53**, 1288 (1988).

[12]G. J. Whaley and P. I. Cohen, in *Layered Structures, Heteroepitaxy, Superlattices, Strain and Metastability,* edited by B. W. Dodson, L. J. Schowalter, J. E. Cunningham, and F. H. Pollak, MRS Symposia Proceedings No. 160 (Materials Research Society, Pittsburgh, 1990), p. 35; Appl. Phys. Lett. **57**, 144 (1990).

[13]P. R. Berger, K. Chang, P. Bhattacharya, J. Singh, and K. K. Bajaj, Appl. Phys. Lett. **58**, 684 (1988).

[14]C. W. Snyder, B. G. Orr, D. Kessler, and L. M. Sander, Phys. Rev. Lett. **66**, 3032 (1991); C. W. Snyder, D. Barlett, B. G. Orr, P. K. Bhattacharya, and J. Singh, J. Vac. Sci. Technol. B **9**, 2189 (1991); C. W. Snyder, J. F. Mansfield, and B. G. Orr, Phys. Rev. B **46**, 9551 (1992).

[15]M. Gendry, V. Drouot, C. Santinelli, and G. Hollinger, Appl. Phys. Lett. **60**, 2249 (1992).

[16]M. Gendry, V. Drouot, C. Santinelli, G. Hollinger, D. Miossi, and M. Pitaval, J. Vac. Sci. Technol. B **10**, 1829 (1992).

[17]J. L. Lievin and C. G. Fonstad, Appl. Phys. Lett. **A51**, 1173 (1987).

[18]Y. Hida, T. T. Tamagawa, H. Ueba, and C. Tatsuyama, J. Appl. Phys. **67**, 7274 (1990).

[19]G. Bauer and G. Springholz, Vacuum **43**, 357 (1992).

[20]G. Springholz and G. Bauer, in *Semiconductor Heterostructures for Photonic and Electronic Applications,* edited by D. C. Houghton, C. W. Tu, and R. T. Tunj, MRS Symposia Proceedings No. 281 (Materials Research Society, Pittsburgh, in press).

[21]P. Wachter, in *Handbook on the Physics and Chemistry of the Rare Earths,* edited by K. A. Geschneider, Jr. and L. Eyring (North-Holland, Amsterdam, 1979), p. 507.

[22]G. Nimtz, in *Numerical Data and Functional Relationships in Science and Technology,* edited by K. Hellwege and O. Madelung, Landolt-Börnstein, New Series, Group III, Vol. 17, Pt. F (Springer-Verlag, Berlin, 1993), p. 168.

[23]J. W. Matthews and A. F. Blakeslee, J. Cryst. Growth **27**, 118 (1974); in *Epitaxial Growth,* edited by A. H. Alper, J. L. Margrave, and A. S. Nowick (Academic, New York, 1975), Pt. B.

[24]E. J. Fantner, H. Clemens, and G. Bauer, in *Advances in X-ray Analysis,* edited by J. B. Cohen, J. C. Russ, P. E. Leyden, C. S. Barett, and P. K. Predecki (Plenum, New York, 1984), Vol. 27, p. 171.

[25]J. C. Bean, L. C. Feldmann, A. T. Fiory, S. Nakahura, and I. K. Robinson, J. Vac. Sci. Technol. A **2**, 436 (1984).

[26]See, for example, M. G. Lagally, D. E. Savyge, and M. C. Tringides, in *Reflection High Energy Electron Diffraction and Reflection Electron Imaging of Surfaces,* edited by P. K. Larsen and P. J. Dobson, Vol. 188 of *NATO Advanced Study Institute Series X* (Plenum, New York, 1988), p. 139.

[27]U. Korte and G. Meyer-Ehmsen, Surf. Sci. **232**, 367 (1990).

[28]E. Bauer, in *Techniques of Metals Research,* edited by R. F. Bunshan (Wiley, New York, 1969), p. 501.

[29]B. Bölger, P. K. Larsen, and G. Meyer Ehmsen (Ref. 26), p. 201.

[30]See, for example, J. M. Van Hove and P. I. Cohen, J. Cryst. Growth **81**, 13 (1987).

[31]D. J. Eaglesham and M. Cerullo, Phys. Rev. Lett. **64**, 1943 (1990).

[32]P. M. J. Marée, K. Nakagawa, F. M. Mulders, J. F. van der Veen, and K. L. Kavanagh, Surf. Sci. **191**, 305 (1987).

[33]B. G. Orr and C. J. Snyder, in *Evolution of Surface and Thin Film Microstructures,* edited by H. A. Atwater, M. Grabow, E. Chason, and M. Lagally, MRS Symposia Proceedings No. 280 (Materials Research Society, Pittsburgh, 1992).

[34]B. W. Dodson and J. T. Tsao, Appl. Phys. Lett. **51**, 1325 (1987).

[35]G. L. Price, Phys. Rev. Lett. **66**, 469 (1990).

[36]B. A. Fox and W. A. Jesser, J. Appl. Phys. **68**, 2801 (1990).

[37]A. Marti Ceschin and J. Massies, J. Cryst. Growth **114**, 693 (1991).

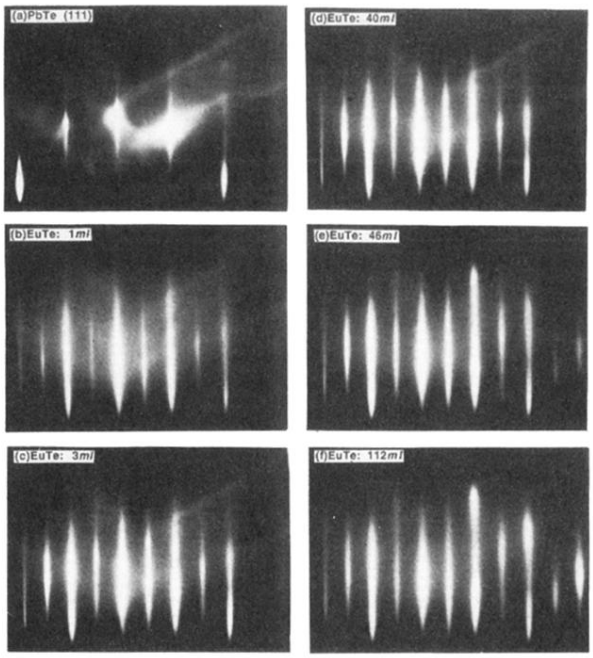

FIG. 3. RHEED patterns of EuTe on PbTe(111) at different stages of growth: (a) for the initial PbTe surface; (b) after 1 ML EuTe, (c) after 3 ML EuTe, (d) after 40 ML EuTe (just before the critical layer thickness $h_c = 45$ ML); (e) after 46 ML EuTe (just after $h_c = 45$ ML); and (f) after 112 ML EuTe. Diffraction conditions: $[1\bar{1}0]$ azimuth and angle of incidence of 1.2°.